as before. The difference between the pulse-height spectra for N_1 and N_2, normalized in the same way as before, is shown in Fig. 6.

The shape of the curve shown in Figs. 5 and 6 indicates that, for equal intensities and bandwidths, the synchrotron-radiation spectrum is less correlated than the thermal spectrum, and the degree of correlation of the synchrotron-radiation photons increases with increasing number of radiating particles.

6. CONCLUSIONS

The foregoing results lead to the following conclusions:

1. For equal mean intensities, thermal radiation has a higher degree of correlation than synchrotron radiation.

2. The degree of correlation of synchrotron radiation increases with increasing number of radiating electrons.

3. The efficiency of recording multiphoton pulses was found to be greater than predicted by the existing theory of photoelectric detection.

4. Analysis of the photomultiplier pulse-height spectra can be used to detect correlations in low-intensity fluxes with characteristic times of $\sim 10^{-11}$–10^{-12} sec.

5. Analysis of the pulse-height spectra produced by a photomultiplier can be effectively used to determine the statistical properties of an unknown source of radiation by comparing the resulting signal with the signal from a source with known statistical properties.

[1]J. R. Klauder and E. C. G. Sudarshan, Fundamentals of Quantum Optics, a), p. 44; b) p. 244; c) p. 318, (Russ. Transl. Mir, M., 1972).
[2]Intern. Symposium of Synchrotron Radiation Users, Daresbury, January 4–7, 1973. Proc. Daresbury Nuclear Physics Laboratory, 1973.
[3]Yu. N. Grigor'ev, I. A. Grishaev, A. N. Dovbnya, A. S. Zelencher, O. G. Il'in, I. I. Koba, V. P. Kozin, S. G. Kononenko, N. I. Mocheshnikov, A. A. Rakityanskiĭ, L. V. Reprintsev, A. S. Tarasenko, B. A. Terekhov, V. D. Tkachenko, A. E. Tolstoĭ, S. D. Faĭnzil'berg, and A. M. Shenderovich, At. Energ. 23, 531 (1967).
[4]R. Glauber, in: Quantum Optics and Quantum Electronics, ed. by O. V. Bogdankevich and O. N. Krokhin (Russ. Transl., Mir, M., 1966, p. 204).
[5]I. A. Grishaev, N. N. Naugol'nyĭ, L. V. Reprintsev, A. S. Tarasenko, and A. M. Shenderovich, Zh. Eksp. Teor. Fiz. 59, 29 (1970) [Sov. Phys. JETP 32, 16 (1971)].
[6]G. Lachs, Phys. Rev. 138, 1012 (1965).
[7]I. R. Gulakov, A. M. Lyutsko, A. I. Pertsev, and M. B. Sadunkovich, Prib. Tekh. Éksp. No. 3, 209 (1970).
[8]I. S. Guk, A. N. Dovbiya, and A. S. Tarasenko, Prib. Tekh. Éksp. No. 2, 192 (1974).
[9]L. Janossy, Zh. Eksp. Teor. Fiz. 28, 679 (1955) [Sov. Phys. JETP 1, 520 (1955)]
[10]V. V. Artem'ev, Radiotekh. Élektron. 13, 316 (1968).

Translated by S. Chomet

Nonlinear quenching of the fluorescence of high-density localized electron excitations in molecular crystals

V. A. Benderskiĭ, V. Kh. Brikenshteĭn, M. A. Kozhushner, I. A. Kuznetsova, and P. G. Filippov

Institute of Chemical Physics, USSR Academy of Sciences, Moscow

(Submitted September 3, 1975)
Zh. Eksp. Teor. Fiz. 70, 521–530 (February 1976)

An investigation was made of the reduction in the quantum efficiency of the fluorescence of pyrene crystals (nonlinear quenching) observed when the optical pumping rate was increased in the range 10^{25}–10^{28} cm^{-3}·sec^{-1} at thermostat temperatures 4.2–300°K and the concentration of excitations reached 10^{-3}–10^{-2} of the density of molecules in a crystal. At 300°K this nonlinear quenching could be described by a model of bimolecular diffusion-controlled recombination. The excimer–excimer annihilation constant was found to be $(4\pm1)\times10^{-11}$ cm^3·sec^{-1}. Below 77°K, when the diffusion of excitations was negligible, the nonlinear quenching was due the dipole-dipole interaction of localized excitations. A model was developed on the basis of averaging of the kinetic equations for the random distribution and it was found that the nonlinear quenching could be described by introducing average self-consistent population. A good agreement was obtained between the experimental and theoretical dependences of the nonlinear quenching on the pumping rate and the effective radius (15–20 Å) was found for the dipole-dipole interaction between eximers.

PACS numbers: 61.40.Km, 78.60.Dg

INTRODUCTION

Reduction in the quantum efficiency of the fluorescence of molecular crystals with rising optical pumping rate, called the nonlinear quenching, was discovered[1] and investigated in detail[2,3] in anthracene crystals. This quenching was attributed in [2,3] to the bimolecular interaction between excitons as a result of which one of the excitons is transferred to a higher vibronic state at the expense of the energy of a second exciton and this is

Copyright © 1976 American Institute of Physics

followed by nonradiative decay of the higher vibronic state into a lower-band exciton and phonons. The nonlinear quenching of excitons is described using the bimolecular diffusion kinetics. However, this description is inappropriate when there is no diffusion of excitations, which is true of impurity crystals or crystals with exciton traps at low temperatures. A suitable object for investigating the nonlinear quenching of localized excitations is a pyrene crystal in which optical transitions produce long-lived complexes formed from excited and unexcited molecules and known as excimers.[4] Excimers are characterized by a low diffusion coefficient (at 77 °K this coefficient is $D \sim 10^{-8}$ $cm^2 \cdot sec^{-1}$ [5]), i.e., the lifetime of an excitation at rest is greater than its radiative lifetime. Moreover, the strong molecular absorption ($\geq 5 \times 10^4 cm^{-1}$) in the near ultraviolet and the high quantum efficiency of the excimer fluorescence (0.64 and 1.0 at 300 °K and below 77 °K, respectively[4]) make it relatively easy to establish high excimer concentrations (10^{-3}–10^{-2} of the density of molecules) in pyrene crystals (these concentrations are needed for investigating the nonlinear quenching of localized excitations). Since the nature of the nonlinear quenching has not yet been studied theoretically, we shall report the experiments and then develop a suitable theory.

EXPERIMENTAL METHOD

Pyrene crystals were grown from the vapor phase by a method used earlier to grow perfect anthracene crystals.[3,7] Pyrene was first purified by multiple recrystallization and subsequent zone melting (60 passes). The purity was deduced from the excimer fluorescence decay time, which was 1.20×10^{-7} sec and 1.92×10^{-7} sec at 300 °K and 4.2 °K, respectively, in agreement with the results reported in[4] for crystals of high degree of purity. Plane-parallel platelets, 10–30 μ thick, were placed in paper envelopes for the excitation and observation of fluorescence from the rear face and mounted on a heat sink of a helium thermostat with a controlled bath temperature between 4.2 °K and 300 °K. The crystals were excited with nitrogen laser ($\lambda = 3371$ Å) pulses of 10 nsec duration (midamplitude), 3 kW power, and 25 Hz repetition frequency. The absolute value of the pulse energy was

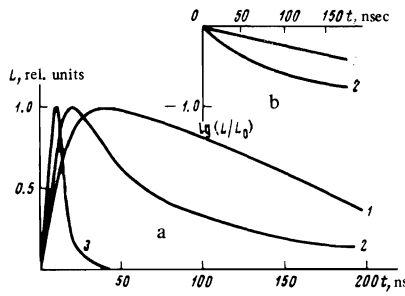

FIG. 1. a) Shape of fluorescence pulses emitted from pyrene crystals subjected to illumination of different intensities: 1) $I_0 = 2 \times 10^{20}$ $cm^{-2} \cdot sec^{-1}$; 2) $I_0 = 2 \times 10^{23}$ $cm^{-2} \cdot sec^{-1}$; 3) shape of pump pulse. The bath temperature was 4.2 °K. b) Determination of the effective decay time during the initial stage.

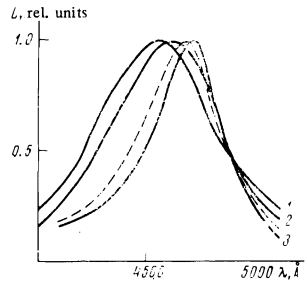

FIG. 2. Fluorescence spectrum of a pyrene crystal at 300 °K (curve 1), 77 °K (2), and 4.2 °K (3). The dashed curve represents the spectrum obtained for $I_0 = 2 \times 10^{23}$ $cm^{-2} \cdot sec^{-1}$ and bath temperature of 4.2 °K.

measured with a thermopile (with an error less than 20%) and the intensity of light was determined from the shape of the laser pulses measured with a fast-response photocell. When the focusing spot diameter was 0.8 mm, the maximum intensity of light (number of photons) incident on a sample was 2×10^{23} $cm^{-2} \cdot sec^{-1}$. A set of calibrated glass plates was used as attenuators by means of which the optical pumping rate could be varied within four orders of magnitude. The fluorescence passed through a set of calibrated neutral filters in such a way that a FÉU-36 photomultiplier (time resolution 5 nsec at mid amplitude) operated as a linear detector. The photomultiplier pulses were applied to a S7-5 stroboscopic oscillator and were plotted by a X–Y recorder. The shape of the fluorescence pulses was determined at various pumping rates (Fig. 1). We measured the pulse amplitude (peak fluorescence intensity), the area under the pulses (light sum), and effective decay time during the initial stage (Fig. 1). We investigated 15 crystals and obtained results which were reproducible from sample to sample.

The absorption coefficient of a pyrene crystal at the excitation wavelength was determined from the dependence of the optical density of mirror-like evaporated films and their thickness at low pumping rates. This coefficient was 8×10^4 and 6×10^4 cm^{-1} at 300 and 4.2 °K, respectively. The fluorescence spectrum of pyrene (Fig. 2) consisted of a wide structure-free (right down to helium temperatures) band associated with the large number of the initial and final states of the optical transitions in excimers.[6] The position of this maximum and the band width varied with temperature, which was used as an internal thermometer in the determination of the temperature of the excited part of the crystal, in a manner similar to the width of the exciton bands and the Debye–Waller factor of impurity bands used for a similar purpose in the case of anthracene crystals.[3,7] When the illumination intensity was 2×10^{23} $cm^{-2} \cdot sec^{-1}$, the adiabatic heating of the absorption layer in a crystal at room temperature (the specific heat of pyrene at 300 °K was 0.4 $cal \cdot g^{-1} \cdot deg^{-1}$), due to the conversion of the excitation energy into heat because of quenching and due to the difference between the pump and fluorescence photon energies, was about 30 °K. When the thermostat temperature was about 4.2 °K, the position of the fluorescence band maximum at the same illumination intensity (dashed curve in Fig. 2) indicated that the temperature in the absorption layer did not exceed 60 °K (because the form of the spectrum changed only slightly below 60 °K, it was not possible to esti-

mate the temperature more exactly). This relatively weak heating was clearly associated with the high thermal diffusivity of perfect pyrene crystals at low temperatures, as found recently for anthracene crystals with a similar crystal structure.[7] Since at the rates of pumping used in our investigations the quantum efficiency and profiles of the fluorescence bands were practically constant between 4.2 °K and 77 °K (i.e., there was no thermal quenching in this range, and the diffusion coefficient even at 77 °K was so small that excimers remained localized), the above change in temperature with pumping rate was ignored.

EXPERIMENTAL RESULTS

Figures 3 and 4 show a reduction in the peak value of the light sum and in the initial fluorescence decay time with rising pumping rate. Since at 300 °K the diffusion coefficient of excimers ($D \approx 10^{-5}$ cm$^2 \cdot$ sec^{-1} [5]) was still sufficient to ensure their mixing during the excitation time (the diffusion length was greater than the average distance between excimers at pumping rates corresponding to quenching), we assumed that the nonlinear quenching at 300 °K could be described by the bimolecular diffusion-controlled recombination mechanism discussed earlier.[1-3] In this case the density of excimers n is described by

$$\frac{dn(x,t)}{dt} = skI(t)e^{-kx} - \frac{n}{\tau_0} - K_{ee}n^2, \tag{1}$$

where $I(t)$ is the shape of the pump pulse; s is the quantum efficiency of the exciton formation process; τ_0 is the exciton lifetime in the absence of nonlinear quenching characterized by the rate constant K_{ee}; k is the absorption coefficient of the pump radiation. If the recombination is diffusion-controlled,[1,2] we have

$$K_{ee} = 8\pi D R_0, \tag{2}$$

where R_0 is the quenching radius, i.e., the distance between excitations for which the annihilation time is equal to the radiative lifetime τ_0. Numerical solution of Eq. (1) and the experimentally determined pulse shape $I(t)$ can be used to find the shape and intensity of the fluorescence pulse:

$$L(t) = \frac{1}{\tau_0}\int_0^\infty n(x,t)\,dx \tag{3}$$

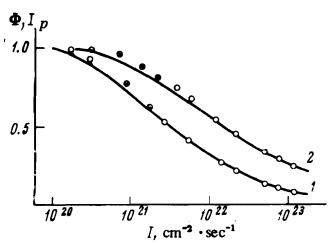

FIG. 3. Dependences of the light sum Φ (curve 1) and peak intensity I_p (curve 2) on the illumination intensity, obtained by a numerical calculation based on Eq. (1). The points are the experimental values obtained at $T = 300$ °K.

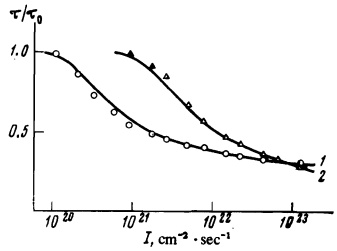

FIG. 4. Dependences of the effective decay time τ/τ_0 on the illumination intensity, found by a numerical calculation based on Eq. (1)—curve 1—and on Eq. (21)—curve 2. The points are the experimental data: ○) obtained at $T = 300$ °K; △) obtained for a bath temperature of 4.2 °K.

as a function of one dimensionless parameter

$$\alpha = K_{ee}kI_0\tau_0^2, \tag{4}$$

where I_0 is the intensity of illumination corresponding to the maximum pumping rate. It is clear from Figs. 3 and 4 that all three experimentally determined characteristics $L(t)$ are in good agreement with calculations. Hence, it follows that at 300 °K the excimer–excimer annihilation process does indeed involve diffusion. Its rate constant, deduced from a comparison of the calculated and experimental results with the aid of Eq. (4), is $(4 \pm 1) \times 10^{-11}$ cm$^3 \cdot$ sec^{-1}, which—for $D = 10^{-5}$ cm$^2 \cdot$ sec^{-1}—corresponds to a quenching radius $R_0 = 17 \pm 4$ Å.

This value of K_{ee} is over three orders of magnitude higher than the value published earlier.[8] The latter value is underestimated, probably because of incorrect determination of the illumination intensity (3×10^{24} cm$^{-2} \cdot$ sec^{-1}) and absorption coefficient ($> 2 \times 10^5$ cm^{-1}), since for these values of k, I_0, and K_{ee} the concentration of excimers would be almost an order of magnitude higher than the density of molecules in a crystal.

Figures 4 and 5 give the low-temperature nonlinear quenching characteristics which are not in agreement with Eq. (1) for any value of K_{ee}. This is further evidence of the unsuitability of the diffusion approach in this case. The localization of excitations alters the nature of the nonlinear quenching process and a different model is not needed.

THEORETICAL MODEL

As pointed out earlier, two excimers annihilate due to the dipole–dipole interaction, whose Hamiltonian can

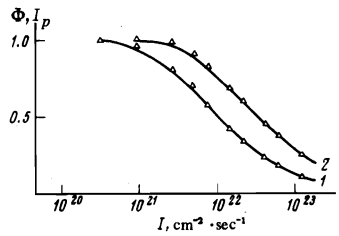

FIG. 5. Dependences of the light sum (curve 1) and peak fluorescence intensity (curve 2) on the illumination intensity found by a numerical calculation based on Eq. (21). The points are the experimental data obtained for a bath temperature of 4.2 °K.

be expressed in the form (averaging over the angles)

$$\hat{V} \approx [(\hat{d}_i)_{10}(\hat{d}_k)_{12} + (\hat{d}_i)_{12}(\hat{d}_k)_{10}]R_{ik}^{-3}, \quad (5)$$

where $(\hat{d})_{10}$ and $(\hat{d})_{12}$ are the dipole moments of the transitions from the state $|1\rangle$ to the states $|0\rangle$ and $|2\rangle$, respectively; the indices i and k label the individual excimers; R_{ik} is the distance between excimers. We shall assume that the bands due to the optical transitions $(1 \rightarrow 0)$ and $(1 \rightarrow 2)$ are sufficiently wide, or, more exactly,

$$|\hat{V}/\hbar\delta| \ll 1, \quad (6)$$

where δ is the band width. In our case the above inequality is satisfied by a large margin because of the considerable width ($\sim 10^3$ cm^{-1}) of the bands due to transitions to vibrational sublevels of excimers.

We shall introduce population operators of an excimer excited state at a site i, $\hat{\rho}_i$, at two (i and k) sites, $\hat{\rho}_i\hat{\rho}_k$, and so on. Then, for the average values $\bar{\rho}_i = \mathrm{Tr}\rho_i\rho$, where ρ is the density matrix of the system, we find that when Eq. (6) is satisfied,

$$\frac{d\bar{\rho}_i}{dt} = -\sum_{k\neq i}\gamma\left(\frac{R_0}{R_{ik}}\right)^6 \overline{\rho_i\rho_k} - \overline{\gamma\rho_i}.$$

If each of the excimers interacts with a large number of neighbors, $\bar{\rho}_i$ and $\bar{\rho}_k$ are weakly correlated and we can write $\overline{\rho_i\rho_k} = \bar{\rho}_i\bar{\rho}_k$. This approximation is invalid for isolated pairs when the correlation between $\bar{\rho}_i$ and $\bar{\rho}_k$ is considerable. However, the probability w that a pair of excimers separated by a distance R is isolated is $w \approx \exp(-2n_0\frac{4}{3}\pi R^3)$. Thus, pairs can be regarded as isolated only for $R \ll \frac{1}{2}n_0^{-1/3}$, i.e., when their number is small. Therefore, in the case of $\bar{\rho}_i$ (which we shall simply denote by ρ_i), we have the following equations:

$$\frac{d\rho_i}{dt} = -\sum_{k\neq i}\gamma\left(\frac{R_0}{R_{ik}}\right)^6 \rho_i\rho_k - \gamma\rho_i, \quad (7)$$

$$\rho_i(\tau_i) = 1, \quad (8)$$

where γ is the rate of annihilation of excimers by radiative and nonradiative transitions. The summation is carried out over all the excimers created up to a moment t and τ_i is the moment of creation of the i-th excimer. The quantity which is observed is

$$n(t) = \sum_i \rho_i(t), \quad (9)$$

which is interpreted as the average number of excitations in a system because the fluorescence intensity $L(t)$ is proportional to this quantity. In the case of localized excitations we find that a closed equation cannot be obtained for $n(t)$ in the presence of annihilation. Therefore, we have to solve the system (7) of nonlinear equations. Such situations can be analyzed by considering the kinetics which allows for the simultaneous interaction of many centers. In an approximate solution of the problem one can use the method of self-consistent population, which to some extent is analogous to the average molecular field method in the theory of phase transitions, i.e., it is assumed that all excitations are in an approximately the same situation relative to one another.

We shall consider the case in which at a moment $t = 0$ a δ-like pump pulse generates all the excitations whose concentration is n_0. It is natural (and agrees with the experimental situation) to assume that excitations are distributed at random and are independent ($\sim 10^{-2}$ of the total number of molecules per unit volume of a crystal is excited). For simplicity and comparison with numerical calculations, we shall ignore also the spontaneous annihilation of excitations, represented by the second term on the right-hand side of Eq. (7). Allowance for this term causes no difficulty. Then, introducing the dimensionless time $(t' = \gamma R_0^6 n_0^2 t)$ and distance $(r' = n_0^{1/3} r)$, we obtain

$$\frac{d\rho_i}{dt'} = -\rho_i\sum_{k\neq i}\frac{1}{|r_{ik}'|^6}\rho_k(t'), \quad \rho_i(0) = 1. \quad (10)$$

The essence of the average self-consistent population method is that all values of $\rho_k(t')$ on the right-hand side of Eq. (10) are replaced by an average population $\bar{\rho}(t')$, which can be found from self-consistency conditions. It follows from Eq. (10) that

$$\rho_i(t') = \exp\left\{-\sum_{k\neq i}\frac{1}{|r_{ik}'|^6}\int_0^{t'}\bar{\rho}(\tau)\,d\tau\right\}. \quad (11)$$

After averaging over the random distribution, carried out in a manner similar to that used in the theory of inductive resonant transport,[9] we obtain the equation for $\bar{\rho}(t')$. It is convenient to introduce

$$\Psi(t') = \int_0^{t'}\bar{\rho}(\tau)\,d\tau, \quad (12)$$

which obeys—in the averaging described above—the equation

$$\frac{d\Psi}{dt'} = \exp\left\{-\left[\frac{16\pi^3}{9}\Psi\right]^{1/2}\right\}, \quad (13)$$

and hence

$$\bar{\rho} = e^{-x(t')}, \quad (14)$$

where $x(t')$ is the solution of the transcendental equation

$$(x-1)e^x = {}^8/_9\pi^3 t' - 1. \quad (15)$$

A graph of $\bar{\rho}(t')$ found from Eqs. (14) and (15), is plotted in Fig. 6.

The average self-consistent population method gives exact results if excitations are distributed in an ordered manner. Then, Eq. (7) [and, consequently, Eq. (11)] is invalid for short time intervals when the closely spaced isolated excitation pairs manage to annihilate. The average self-consistent population method was

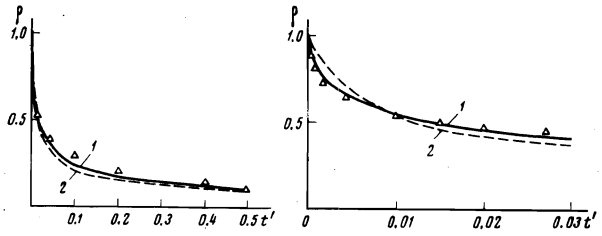

FIG. 6. Decay curves of the average population $\bar{p}$: 1) calculation based on Eqs. (14) and (15); 2) calculation based on Eq. (19). The points represent the results of the numerical solution of the system of equations (10) by the Monte Carlo method.

checked by a numerical calculation of the system (10) for 125 excitations distributed randomly in a cube with $0<x', y', z'<5$. The boundary effects (excitations near a boundary have, on the average, fewer neighbors than in the bulk) were avoided by introducing periodicity conditions: excitations in neighboring cubes were assumed to be distributed exactly as in the cube in which the coordinates of the 125 excitations were selected using tables of random numbers. The size of the memory and the available computer time did not allow us to increase significantly the number of particles so that introduction of periodicity disturbed the randomness of the distribution. The results of this calculation are plotted in Fig. 6. We can see that there is a satisfactory agreement between the average self-consistent population method and numerical calculations. It should be pointed out that as the number of excitations increases [the calculation was also carried out for 27 (in a cube with $0<x', y', z'<3$) and 64 (in a cube with $0<x', y', z'<4$) particles], the calculated curve approached more and more closely the curve found by the average self-consistent population method.

If the duration of a pump pulse creating excimers is comparable with the excimer annihilation time, the kinetic equation obtained by the average self-consistent population method becomes much more complicated because then the dependence of the population of an excited level on time t depends strongly on the moment of creation τ. The equation then becomes

$$\bar{p}(t,\tau)=\exp\left\{-a\int_{-\infty}^{\tau}I(\tau')\left[\int_{\tau}^{t}\bar{p}(t',\tau')dt'\right]^{1/2}d\tau' -a\int_{\tau}^{t}I(\tau')\left[\int_{\tau'}^{t}\bar{p}(t',\tau')dt'\right]^{1/2}d\tau'-\gamma(t-\tau)\right\}, \tag{16}$$

where $a=\frac{4}{3}\pi^{3/2}\gamma^{1/2}ksR_0^3$. The number density of excitations is

$$n(t)=ks\int_{-\infty}^{t}I(\tau)\bar{p}(t,\tau)d\tau. \tag{17}$$

If the pulse is very short, Eq. (16) naturally reduces to Eq. (11). In the steady-state case we have $\bar{p}(t,\tau)\to\bar{p}(t-\tau)$ and an analysis of the transformed equation (16) gives the following expression for the steady-state density of excitations under nonlinear quenching conditions:

$$n\propto I^{1/2}. \tag{18}$$

This result can also be obtained by dimensional analysis. The only parameters which govern the system are the optical pumping rate kI of dimensions $cm^{-3}\cdot sec^{-1}$ and the product γR_0^6 of dimensions $cm^6\cdot sec^{-1}$. From them we can find unambiguously a quantity whose dimensions are of concentration $n\propto(\gamma R_0^6)^{-1/3}(kI)^{1/3}\propto I^{1/3}$. It should be noted that this result is related to the dipole–dipole nature of the interaction between excitations.

It is not possible to solve analytically Eq. (16) and even a numerical solution is difficult to obtain. Therefore, we shall try to find a simpler expression directly for the annihilation part dn/dt so as to be able to solve a differential (and not a complex integral) kinetic equation. We note first that Eq. (18) is obtained from the steady-state solution of the equation

$$dn/dt=-\beta n^3+I. \tag{19}$$

In fact, the rate of annihilation is

$$\propto\sum_{k}\frac{1}{r_{ik}^6}$$

and, if we assume that the number of nearest excited neighbors of any excitation is proportional to the density of these neighbors, we find that $1/r_{ik}\propto n^2$ and, consequently, $(dn/dt)_{ann}\propto n^3$. A suitable selection of the coefficient β makes it possible to represent the annihilation term in such a way that in the case of pulse creation of excitations we obtain $n(t)$ which is close to the exact solution. It is clear from Fig. 6 that this can be done by selecting

$$\beta=115\gamma R_0^6. \tag{20}$$

One should avoid attributing too deep a meaning to this approximation. It is of a form which implies some effective mixing of excitations in the system, although it follows from the conditions of the problem that this is not true. We shall show in the next section that some characteristic and unexpected features of the exact kinetics (which, unfortunately, cannot yet be checked experimentally) are not given by this approximation. Under the experimental conditions employed, the introduction of such "cubic" annihilation of excitations makes it possible to obtain the following simple differential equation:

$$dn/dt=skI(t)e^{-kz}-n/\tau-\beta n^3. \tag{21}$$

We used Eq. (21) and $I(t)$, which was the experimental shape of the pump pulse, to find numerically the dependences of the following quantities on the illumination intensity: 1) quenching at the fluorescence pulse maximum; 2) the fluorescence light sum; 3) the shape of a fluorescence pulse. All three characteristics were found to be in good agreement with the experimental results when only one parameter β was suitably adjusted and this, in our opinion, was evidence of ade-

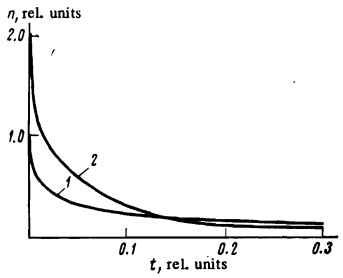

FIG. 7. Decay curves $n(t)$ plotted for $n_0 = 1$ (curve 1) and $n_0 = 2$ (curve 2).

quacy of the theoretical representations. The value of R_0 found from Eq. (21) was 17 ± 3 Å.

DISCUSSION OF RESULTS

We have shown above that in two limiting cases (fast diffusion of excitations and rigorously localized excitations) the nonlinear quenching of the fluorescence of molecular crystals is described by two different dependences of the fluorescence intensity and of its decay time on the optical pumping rate, as represented by Eqs. (1) and (21). The only quenching characteristic linking the two limiting cases is the quenching radius R_0.

We shall first consider the range of diffusion coefficients and excitation densities in which Eq. (1) is valid. The time taken to diffuse a distance equal to the average separation between excitations should be less than the characteristic time of the dipole–dipole annihilation for the same excitation density:

$$D/6r^2 < \beta/r^6, \qquad (22)$$

where $r = (\frac{4}{3}\pi n_0)^{-1/3}$ and n_0 is the density of excitations in the absence of quenching. For $n_0 = 10^{19}$ and 10^{20} cm^{-3}, the diffusion coefficient D should be greater than 4×10^{-8} and 10^{-6} cm$^2 \cdot$ sec^{-1}, respectively, which is satisfied well at $T = 300$ °K but not at $T < 60$ °K. Consequently, in an analysis of the experimental results we have to use two different theoretical models. Our low-temperature experimental data do not reveal interesting features of the kinetics of quenching of localized excitations because the pump pulses are too long. In the case of instantaneous creation of excitations the asymptotic solution (15) in the absence of monomolecular annihilation ($\gamma = 0$) is of the form $\bar{\rho} \propto 1/t'$, whereas experimental observations give $n(t) = n_0 \bar{\rho}(t) \approx 1/n_0 t$.

Thus, beginning from a certain moment, the value of $n(t)$ decreases with rising n_0. This behavior of $n(t)$ can readily be deduced from the form of curves 1 and 2 in Fig. 7. This unusual kinetic result is associated with the memory effect in systems which exhibit multipole interaction in the absence of excitation mixing. The evolution of such a system with time depends on the initial density of excitations throughout the lifetime of the system since a spatial distribution of excitations is random only initially. On the other hand, in the case of spatial mixing of excitations the kinetics of the decay is governed only by the instantaneous density of excitations and not by their distribution.

These features are not revealed in the case of long pump pulses and monomolecular decay. The asymptote of the solution of Eq. (21), which is $\sim 1/\sqrt{t}$ for $\gamma = 0$, does not agree with the true asymptote ($\sim 1/t$), but if $\gamma \neq 0$ this difference can be ignored in practice. For this reason only the initial part of the fluorescence decay is compared with the theory because in this case Eq. (21) is sufficiently rigorous.

We are grateful to N. I. Peregudov and V. A. Volodin for a numerical solution of the system of equations (10) by the Monte Carlo method.

[1]N. A. Tolstoĭ and A. P. Abramov, Fiz. Tverd. Tela (Leningrad) 9, 340 (1967) [Sov. Phys.-Solid State 9, 255 (1967)].
[2]S. D. Babenko, V. A. Benderskii, V. I. Goldanskii, A. G. Lavrushko, and V. P. Tychinskii, Phys. Status Solidi B 45, 91 (1971).
[3]O. S. Avanesyan (Avanesjan), V. A. Benderskii, V. Kh. Brikentsein, V. L. Broude, L. I. Korshunov, A. G. Lavrushko, and I. I. Tartakovskii, Mol. Cryst. Liq. Cryst. 29, 165 (1974).
[4]J. B. Birks, A. A. Kazzaz, and T. A. King, Proc. R. Soc. Ser. A 291, 556 (1966).
[5]M. Tomura and Y. Takahashi, J. Phys. Soc. Jpn. 31, 797 (1971).
[6]J. B. Birks and I. H. Munro, "The fluorescence lifetimes of aromatic molecules," Prog. React. Kinet. 4, 239 (1967).
[7]V. A. Benderskii, V. Kh. Brikenshtein (Brikenstein), V. L. Broude, and A. G. Lavrushko, Solid State Commun. 15, 1235 (1974).
[8]E. D. Vol, V. A. Goloyadov, L. S. Kukushin, Yu. V. Naboikin, and N. B. Silaeva, Phys. Status Solidi B 47, 685 (1971).
[9]T. Förster, Ann. Phys. (Leipzig) 2, 55 (1948); Discuss. Faraday Soc. No. 27, 7 (1959).

Translated by A. Tybulewicz